Estimation of Cold Characteristics for Fundamental-Mode MBK Cavities

Khanh T. Nguyen
Beam-Wave Research, Inc., Bethesda MD 20814

David K. Abe
U.S. Naval Research Laboratory, Code 6840
Washington, DC 20375

Dean E. Pershing
ATK Mission Research
Newington, VA 22122

Baruch Levush
U.S. Naval Research Laboratory, Code 6840
Washington, DC 20375

Abstract: *We describe the development of simple formulae to accurately estimate the R/Q's in single-gap, fundamental-mode MBK cavities and to describe their sensitivity to radius and frequency. These equations can be very useful in the initial design process and can lead to robust cavity designs that are relatively insensitive to manufacturing tolerances.*

Keywords: Multiple-beam klystron; MBK; single-gap cavity; *R/Q*.

Introduction

Fundamental-mode MBKs employ re-entrant cavities to achieve high values of *R/Q* for effective beam-wave interaction. Figure 1 illustrates the general geometry of such cavities. While similar to single-beam klystron cavities, fundamental-mode MBK cavities have two key differences. First, to accommodate multiple beamlets, the radius of the interaction gap nose, *a*, tends to be much larger than the interaction gap width, *d*. Second, due to their relatively small diameters, individual beam tunnels are highly cut-off, and consequently fringing RF fields are relatively negligible. The large *a/d* aspect ratio can cause substantial variation in the *R/Q*'s experienced by individual beamlets depending on their radial position within the interaction nose. Moreover, for broadband devices, this variation is frequency dependent.

Model Development

We have used Maxwell's equations and Kirchoff's law along with the appropriate matching boundary conditions to derive the radial profiles of the axial electric field and the on-axis values of *R/Q*, which are summarized below. To simplify the problem, we have taken advantage of the fact that the individual beam tunnels are highly cut-off, allowing us to approximate the interaction gap noses as parallel plates as shown in Fig. 1.

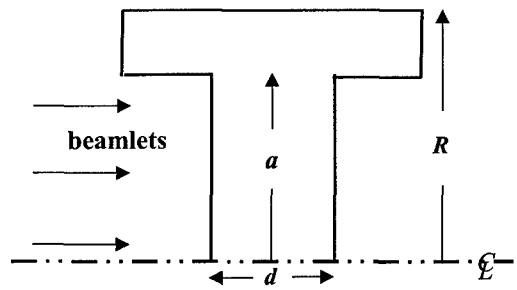

Figure 1. Schematic diagram of a single-gap, re-entrant cavity employed in MBKs.

The radial dependence of the mid-plane RF axial electric field can be expressed as,

$$E_z(r<a) \approx \frac{V_g}{d}\left[J_0(X\frac{r}{a}) + \delta_E e^{\kappa a(r/a - 1)}\right]$$

$$E_z(r>a) \approx \frac{V_g}{d} J_0(X)\left(1+\frac{d}{R-a}\right)\times \left[\frac{1}{r-(a-d)} - \frac{1}{R-(a-d)}\right] + \frac{V_g}{d}\delta_E e^{\kappa a(1-r/a)}, \quad (1)$$

where V_g is the on-axis gap voltage; $X = \omega\, a/c$; ω is the angular frequency; c is the speed of light in vacuum; and δ_E is the magnitude of the contribution from the effect of edge perturbation effect, which can be approximated by

$$\delta_E = -J_0(X)\left[\frac{a}{d}\left(1+\frac{d}{R-a}\right) - \frac{XJ_1(X)}{J_0(X)}\right]\frac{1}{2\kappa a}. \quad (2)$$

In the above equations, J_0 and J_1 are the zero- and first-order Bessel functions, respectively, and we define

1-4244-0108-9/06/$20.00 © 2006 IEEE

$$\kappa a = \left(\frac{\pi a^2}{d^2} - X^2 \right)^{1/2} . \qquad (3)$$

The on-axis R/Q is described by

$$\left(\frac{R}{Q} \right)_0 = \left(\frac{d}{\omega_0 \varepsilon_0 (\pi a^2)} \right) \times \left[\frac{2J_1(X)}{X} - J_0(X) \left(\frac{a}{d} \left(1 + \frac{d}{R-a} \right) - \frac{XJ_1(X)}{J_0(X)} \right) \frac{1}{(\kappa a)^2} \right]^{-1}, \qquad (4)$$

where ω_0 is the cavity resonant angular frequency, and ε_0 is the permittivity of free space. Finally, the variation of R/Q with radial distance can be expressed as

$$\frac{R}{Q} \approx \left(\frac{R}{Q} \right)_0 \left[J_0(X \frac{r}{a}) + \frac{2}{\pi} \delta_E e^{\kappa a (r/a - 1)} \right]. \qquad (5)$$

Model Validation

To compare and validate (1)-(5), we have simulated a series of test cavities with the electromagnetics code, HFSS. For example, Fig. 2 plots comparisons between (1) and the HFSS simulated results for the mid-plane axial electric field for three cavity gap widths. As can be seen in the figure, the agreement is very good. In particular, note the sharp drop-off of the axial electric field as the gap width is increased. Comparisons between the HFSS computations of the on-axis R/Q values for the three cases shown in Fig. 2 and estimates using (2) are summarized in Table 1; once again the analytic formula is in good agreement with the simulations. These comparisons demonstrate the utility of these formulae as a tool for estimating the cold MBK re-entrant cavity characteristics. Detailed derivations will be described and discussed in the full presentation.

Table 1. Comparison of theoretical and HFSS-simulations of on-axis R/Q for the parameters given in Fig. 2.

d (cm)	R/Q (theory)	R/Q (HFSS)
0.5	36.1	34.1
0.7	47.5	46.1
0.9	58.7	59.1

Acknowledgement

This work was supported by the Office of Naval Research.

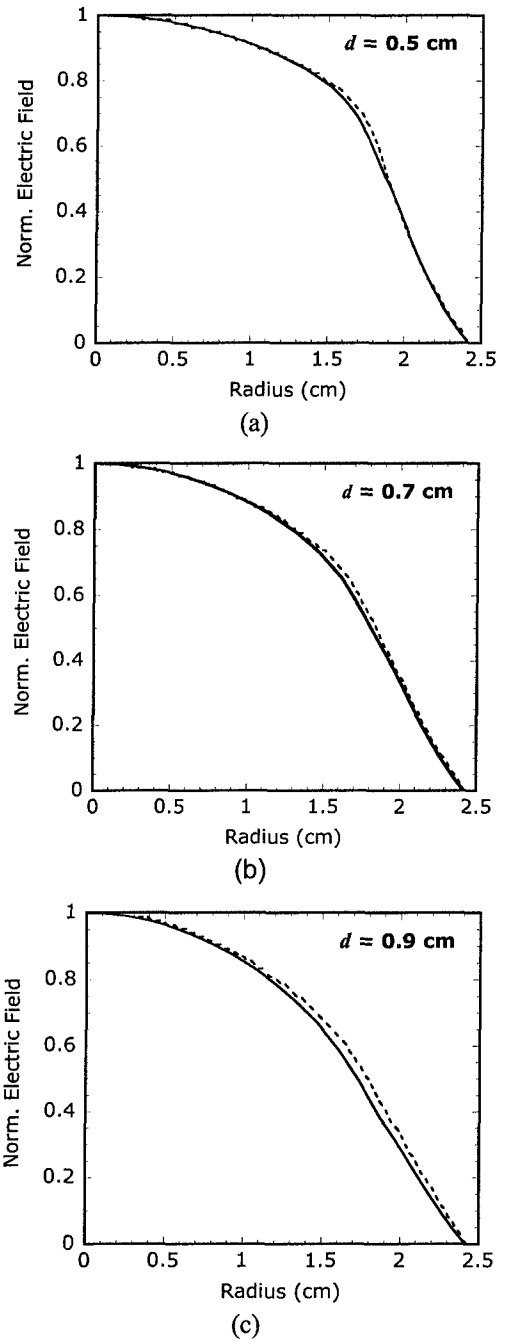

Figure 2. Comparison of analytic (solid) and HFSS-simulated (dashed) radial profiles of the axial electric field at the mid-plane of the cavity gap for (a) d = 0.5 cm; (b) d = 0.7 cm; and (c) d = 0.9 cm (a = 1.84 cm and R = 2.42 cm in all cases).